

Chiral-glass transition and replica symmetry breaking of a three-dimensional Heisenberg spin glass

K. Hukushima

ISSP, Univ. of Tokyo, Roppongi, Minato-ku, Tokyo 106-8666, Japan

H. Kawamura

Faculty of Engineering and Design, Kyoto Institute of Technology, Sakyo-ku, Kyoto 606-8585, Japan

(November 21, 2018)

Extensive equilibrium Monte Carlo simulations are performed for a three-dimensional Heisenberg spin glass with the nearest-neighbor Gaussian coupling to investigate its spin-glass and chiral-glass orderings. The occurrence of a finite-temperature chiral-glass transition without the conventional spin-glass order is established. Critical exponents characterizing the transition are different from those of the standard Ising spin glass. The calculated overlap distribution suggests the appearance of a peculiar type of replica-symmetry breaking in the chiral-glass ordered state.

While experiments have provided convincing evidence that spin-glass (SG) magnets exhibit an equilibrium phase transition at a finite temperature, the true nature of the experimentally observed SG transition and that of the low-temperature SG phase still remain open problems [1]. A simple Ising model has widely been used as a “realistic” SG model in the studies, *e.g.*, of the critical properties of the SG transition, or of the issue of whether the SG state exhibits a spontaneous replica-symmetry breaking (RSB). One should bear in mind, however, that the magnetic interactions in many SG materials are nearly isotropic, being well described by an isotropic Heisenberg model, in the sense that the magnetic anisotropy is considerably weaker than the exchange interaction. In apparent contrast to experiments, numerical simulations have indicated that the standard spin-glass order occurs only at zero temperature in the three-dimensional (3D) Heisenberg SG [2–6]. Although the magnetic anisotropy inherent to real materials is often invoked to explain this apparent discrepancy with experiments, it still remains puzzling that no detectable sign of Heisenberg-to-Ising crossover has been observed in experiments which is usually expected to occur if the observed finite-temperature transition is caused by the weak magnetic anisotropy [1,2].

In order to solve this apparent puzzle, a chirality mechanism of experimentally observed spin-glass transitions was proposed by one of the authors [3]. This scenario is based on the assumption that an isotropic 3D Heisenberg SG exhibits a finite-temperature *chiral-glass* transition without the conventional spin-glass order, in which only spin-reflection symmetry is broken with preserving spin-rotation symmetry. Chirality is an Ising-like multi-spin variable representing the sense or the handedness of the noncollinear spin structures induced by spin frustration. In this scenario, all essential features of many of real SG transitions and SG ordered states should be determined by the properties of the chiral-glass transition and of the chiral-glass state *in the fully isotropic system*, while the role of the magnetic anisotropy is secondary which “mixes” the spin and the chirality and “reveals”

the chiral-glass transition as an anomaly in experimentally accessible quantities.

Numerical studies on the 3d XY spin glasses have given strong support to the occurrence of a finite-temperature chiral-glass transition [8–10]. In the Heisenberg case, while previous numerical works agreed in that the standard SG order occurred only at $T = 0$, the question whether there really occurs a finite-temperature chiral-glass order has remained inconclusive [3,4]. Very recently, an off-equilibrium Monte Carlo simulation by one of the authors has given evidence for the occurrence of a finite-temperature chiral-glass order in the 3D Heisenberg SG [5]. However, the full critical properties of the chiral-glass transition as well as the properties of the chiral-glass ordered state itself, particularly the question of the possible RSB, still remains largely unclear. In this Letter, we perform extensive *equilibrium* Monte Carlo simulations of a 3D Heisenberg SG in order to determine the detailed static and dynamic critical properties and to clarify the nature of the chiral-glass ordered state.

Our model is the classical Heisenberg model on a simple cubic lattice with $N = L^3$ spins defined by the Hamiltonian,

$$\mathcal{H} = - \sum_{\langle ij \rangle} J_{ij} \mathbf{S}_i \cdot \mathbf{S}_j, \quad (1)$$

where $\mathbf{S}_i = (S_i^x, S_i^y, S_i^z)$ is a three-component unit vector, and the sum runs over all nearest-neighbor pairs. The interactions J_{ij} are random Gaussian variables with zero mean and variance J . The local chirality at the i -th site and in the μ -th direction, $\chi_{i\mu}$, is defined for *three* neighboring spins by the scalar [2,4],

$$\chi_{i\mu} = \mathbf{S}_{i+\hat{e}_\mu} \cdot (\mathbf{S}_i \times \mathbf{S}_{i-\hat{e}_\mu}), \quad (2)$$

where \hat{e}_μ ($\mu = x, y, z$) denotes a unit lattice vector along the μ -axis.

Monte Carlo simulation is performed based on the exchange MC method, sometimes called “parallel tempering”, which turns out to be an efficient method for thermalizing systems exhibiting slow dynamics [7]. By making use of this method, we have succeeded in equilibrating

the system down to the temperature considerably lower than those attained in the previous simulations [2,4]. We run two independent sequences of systems (replica 1 and 2) in parallel, and compute an overlap between the chiral variables in the two replicas,

$$q_\chi = \frac{1}{3N} \sum_{i\mu} \chi_{i\mu}^{(1)} \chi_{i\mu}^{(2)}. \quad (3)$$

In terms of this chiral overlap q_χ , the Binder ratio of the chirality is calculated by

$$g_{CG}(L) = \frac{1}{2} \left(3 - \frac{[\langle q_\chi^4 \rangle]}{[\langle q_\chi^2 \rangle]^2} \right), \quad (4)$$

where $\langle \dots \rangle$ represents the thermal average and $[\dots]$ represents the average over bond disorder. For the Heisenberg spin, one can introduce an appropriate Binder ratio in terms of a tensor overlap $q_{\mu\nu}$ ($\mu, \nu = x, y, z$) which has $3^2 = 9$ independent components [4],

$$q_{\mu\nu} = \frac{1}{N} \sum_i S_{i\mu}^{(1)} S_{i\nu}^{(2)} \quad (\mu, \nu = x, y, z), \quad (5)$$

via the relation,

$$g_{SG}(L) = \frac{1}{2} \left(11 - 9 \frac{\sum_{\mu, \nu, \delta, \rho} [\langle q_{\mu\nu}^2 q_{\delta\rho}^2 \rangle]}{(\sum_{\mu, \nu} [\langle q_{\mu\nu}^2 \rangle])^2} \right). \quad (6)$$

The lattice sizes studied are $L = 6, 8, 10, 12$ and 16 with periodic boundary conditions. Equilibration is checked by monitoring the stability of the results against at least three-times longer runs for a subset of samples. Sample average is taken over 1500 ($L = 6$), 1200 ($L = 8$), 640 ($L = 10$), 296 ($L = 12$) and 136 ($L = 16$) independent bond realizations. Note that in the exchange MC simulations the data at different temperatures are correlated. Error bars are estimated from statistical fluctuations over the bond realizations.

The size and temperature dependence of the Binder ratios of the spin and of the chirality, g_{SG} and g_{CG} , are shown in Fig. 1(a) and (b), respectively. As can be seen from Fig. 1(a), g_{SG} constantly decreases with increasing L at all temperatures studied, suggesting that the conventional spin-glass order occurs only at zero temperature, consistent with the previous results [2–6]. Fig. 1(a) reveals that g_{SG} for larger lattices ($L = 10, 12, 16$) exhibits an anomalous bending around $T/J \simeq 0.15$, suggesting a change in the ordering behavior in this temperature range. As can be seen from Fig. 1(b), the curves of g_{CG} for different L tend to merge for larger L in the temperature range where the curves of g_{SG} exhibit an anomalous bending. Furthermore, on increasing L , the merging points gradually move toward higher temperatures, suggesting that the chiral-glass transition indeed occurs at a finite temperature. Since g_{CG} for different L do not cross here at $g_{CG} > 0$, however, it is not necessarily easy to unambiguously locate the chiral-glass transition point, or

even to completely rule out the possibility of only a zero-temperature transition with rapidly growing (*e.g.*, exponentially growing) correlation length. Meanwhile, the calculated g_{CG} shows a negative dip whose depth gradually increases with increasing L , whereas its position gradually shifts toward lower temperature. Note that, if the systems would not exhibit any finite-temperature transition, $g_{CG}(T; L \rightarrow \infty)$ should be equal to zero at any $T > 0$ and to unity at $T = 0$ (for the nondegenerate ground state as expected for the present Gaussian coupling). Since $g_{CG}(T; L \rightarrow \infty)$ is a single-valued function of T , the existence of a negative dip growing with L hardly reconciles with the absence of a finite-temperature transition so long as this tendency persists, and suggests the chiral-glass transition occurring at $T = T_{CG} > 0$ at which g_{CG} takes a *negative* value unlike the standard cases of the 3D Edwards-Anderson (EA) Ising model or the infinite-range Sherrington-Kirkpatrick (SK) model.

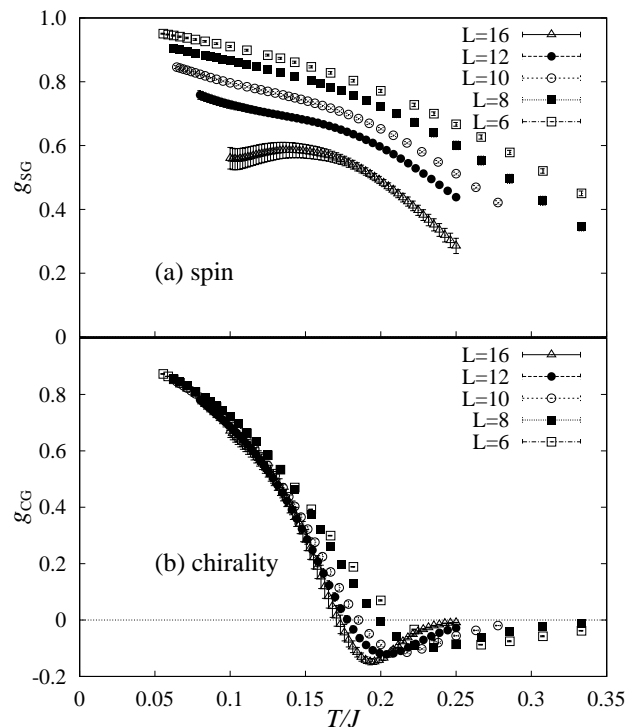


FIG. 1. Temperature and size dependence of the Binder ratios of the spin (a) and of the chirality (b).

More unambiguous estimate of T_{CG} can be obtained from the equilibrium dynamics of the model. Thus, we calculate both the spin and chirality autocorrelation functions defined by

$$C_s(t) = \frac{1}{N} \sum_i [\langle \mathbf{S}_i(t_0) \cdot \mathbf{S}_i(t_0 + t) \rangle], \quad (7)$$

$$C_\chi(t) = \frac{1}{3N} \sum_{i,\mu} [\langle \chi_{i\mu}(t_0) \chi_{i\mu}(t_0 + t) \rangle], \quad (8)$$

where MC simulation is performed according to the standard heat-bath updating here. The starting spin configuration at $t = t_0$ is taken from the equilibrium spin configuration generated in our exchange MC runs.

Monte Carlo time dependence of the calculated $C_s(t)$ and $C_\chi(t)$ are shown in Fig. 2 on log-log plots at several temperatures for $L = 16$. We found no significant difference in the data of $L=12$ and 16 , and the finite-size effect is negligible in our time window. As can be seen from Fig. 2(a), $C_s(t)$ shows a downward curvature at all temperature studied, suggesting an exponential-like decay characteristic of the disordered phase, consistently with the absence of the standard spin-glass order. In sharp contrast to this, $C_\chi(t)$ shows either a downward curvature characteristic of the disordered phase, or an upward curvature characteristic of the long-range ordered phase, depending on whether the temperature is higher or lower than $T/J \simeq 0.16$, while just at $T/J \simeq 0.16$ the linear behavior corresponding to the power-law decay is observed: See Fig. 2(b). Hence, our dynamical data indicates that the chiral-glass order without the standard spin-glass order takes place at $T_{CG}/J = 0.160 \pm 0.005$, below which a finite chiral EA order parameter $q_{CG}^{EA} > 0$ develops. From the slope of the data at $T = T_{CG}$, the exponent λ characterizing the power-law decay of $C_\chi(t) \approx t^{-\lambda}$ is estimated to be $\lambda = 0.193 \pm 0.005$. The estimated T_{CG} is in good agreement with the previous estimate of Ref. [5], $T_{CG}/J = 0.157 \pm 0.01$.

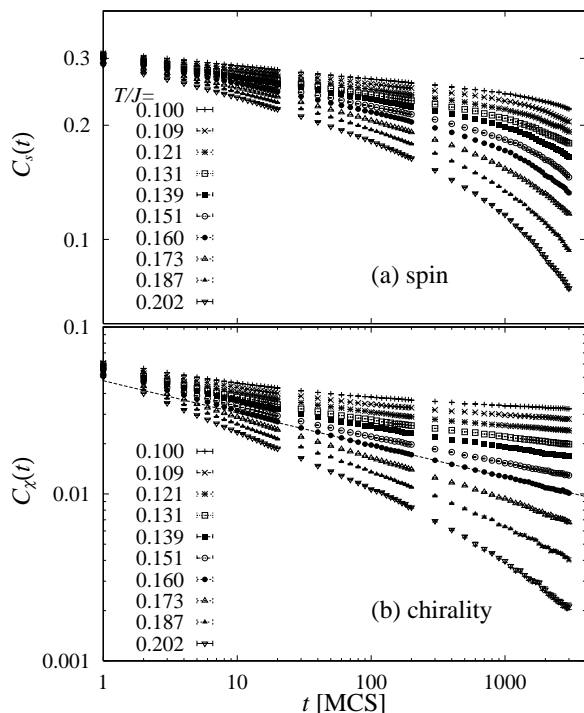


FIG. 2. Log-log plots of the time dependence of the equilibrium spin (a) and chirality (b) autocorrelation functions at several temperatures. The lattice size is $L = 16$ averaged over 64 samples. In (b), the best straight-line fit is obtained at $T/J = 0.16$, represented by the broken line.

The behavior of the chiral-glass order parameter, or the associated chiral-glass susceptibility $\chi_{CG} = 3N[\langle q_\chi^2 \rangle]$, turns out to be consistent with this. In the inset of Fig. 3, we show the reduced chiral-glass susceptibility $\tilde{\chi}_{CG} \equiv \chi_{CG}/\bar{\chi}^4$, normalized by the amplitude of the local chirality $\bar{\chi}^2 \equiv (1/3N) \sum_{i,\mu} [\langle \chi_{i\mu}^2 \rangle]$, versus the reduced temperature $t \equiv |(T - T_{CG})/T_{CG}|$ on a log-log plot. From the asymptotic slope of the data, the susceptibility exponent is estimated to be $\gamma_{CG} = 1.5 \pm 0.3$. Note that the estimated susceptibility exponent is significantly smaller than that of the standard 3D Ising EA model, $\gamma \simeq 4$ [1d].

If we combine the present estimate of γ_{CG} with the estimate of β_{CG} from the off-equilibrium simulation of Ref. [5] and use the scaling relations, various chiral-glass exponents can be estimated to be $\alpha \simeq -1.7$, $\beta_{CG} \simeq 1.1$, $\gamma_{CG} \simeq 1.5$, $\nu_{CG} \simeq 1.2$ and $\eta_{CG} \simeq 0.8$. The dynamical exponent is estimated to be $z_{CG} \simeq 4.7$ by using the estimated value of λ and the scaling relation $\lambda = \beta_{CG}/z_{CG}\nu_{CG}$. While the dynamical exponent z_{CG} comes rather close to the z of the 3D EA model, the obtained static exponents differ significantly from those of the 3D Ising EA model $\beta \simeq 0.55$, $\gamma \simeq 4.0$, $\nu \simeq 1.7$ and $\eta \simeq -0.35$ [1d], suggesting that the universality class of the chiral-glass transition of the 3D Heisenberg spin glass differs from that of the standard 3D Ising spin glass. Possible long-range and/or many-body nature of the chirality-chirality interaction might be the cause of this deviation.

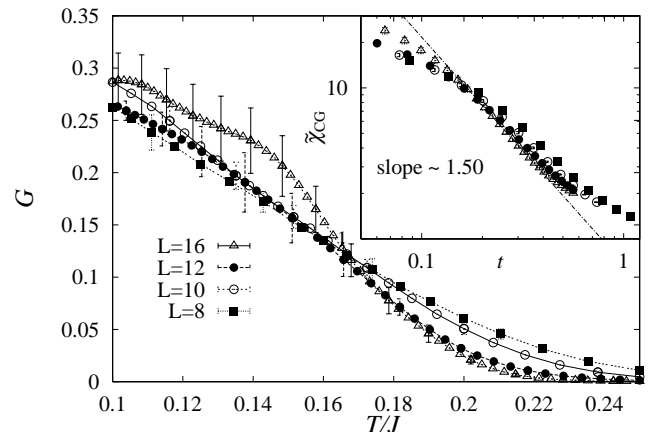


FIG. 3. Temperature and size dependence of the G parameter of the chirality defined by Eq. (9). The inset represents a log-log plot of the reduced chiral-glass susceptibility versus the reduced temperature $t \equiv |(T - T_{CG})/T_{CG}|$.

Further evidence of a phase transition is obtained from the behavior of the G parameter of the chirality defined by

$$G(L) = \frac{[\langle q_\chi^2 \rangle^2] - [\langle q_\chi^2 \rangle]^2}{[\langle q_\chi^4 \rangle] - [\langle q_\chi^2 \rangle]^2}. \quad (9)$$

While this quantity was originally introduced to represent the non-self-averaging character of the system [11],

Bokil *et al* argued that it was not necessarily so [12]. Still, a crossing of $G(L)$ for different L , if it occurs, can be used to identify the transition [12]. As shown in Fig. 3, for $T > T_{CG}$ $G(L)$ decreases with increasing L tending to zero, while for $T < T_{CG}$ it tends to increase with L , thus lending further support to the existence of a phase transition at $T = T_{CG}$.

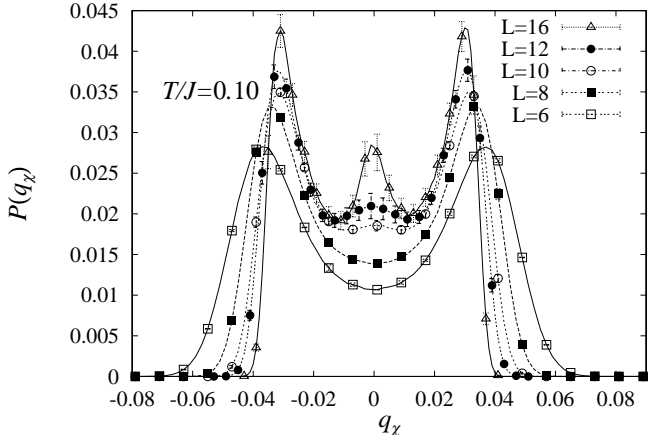


FIG. 4. Chiral-overlap distribution function below T_{CG} . The temperature is $T/J = 0.1$.

In Fig. 4, we display the distribution function of the chiral-overlap defined by $P(q'_\chi) = [\langle \delta(q_\chi - q'_\chi) \rangle]$ calculated at a temperature $T/J = 0.1$, well below the chiral-glass transition temperature. The shape of the calculated $P(q_\chi)$ is somewhat different from the one observed in the standard Ising-like models such as the 3D EA model or the mean-field SK model. As usual, $P(q_\chi)$ has standard “side-peaks” corresponding to the Edwards-Anderson order parameter $\pm q_{CG}^{EA}$, which grow and sharpen with increasing L . The extracted value of $\pm q_{CG}^{EA}$ coincides with that evaluated from the relaxation of $C_\chi(t)$. In addition to the side peaks, an unexpected “central peak” at $q_\chi = 0$ shows up for larger L , which also grows and sharpens with increasing L . This latter aspect, *i.e.*, the existence of a central peak, is a peculiar feature of the chiral-glass ordered state never observed in the EA or SK models. Since we do not find any sign of a first-order transition such as a discontinuity in the energy, the specific heat nor the order parameter q_{CG}^{EA} , this feature is likely to be related to a nontrivial structure in the phase space associated with the chirality. We note that this peculiar feature is reminiscent of the behavior characteristic of some mean-field models showing the so-called *one-step* RSB[1b]. Indeed, the existence of a negative dip in the Binder ratio g_{CG} and the absence of a crossing of g_{CG} at $g_{CG} > 0$ are consistent with the occurrence of such one-step-like RSB [13]. Our data of $P(q_\chi)$ are also not incompatible with the existence of a continuous plateau between $[-q_{CG}^{EA}, q_{CG}^{EA}]$ in addition to the delta-function peaks. According to the chirality mechanism, such novel one-step-like RSB should be realized in the *spin* ordering of real Heisenberg-like spin glasses.

We note that, if $P(q_\chi)$ has a nontrivial structure as suggested from Fig. 4, the denominator of Eq. (9) should remain nonzero at $0 < T < T_{CG}$. Then, our data of $G(L)$ in Fig. 3 indicates that the chiral-glass state is non-self-averaging.

In summary, spin-glass and chiral-glass orderings of the 3D Heisenberg SG are studied by Monte Carlo simulations. Our observation both on statics and dynamics strongly suggests the existence of a stable chiral-glass phase at finite temperatures without the conventional spin-glass order. This fact strengthens the plausibility of the chirality mechanism for experimentally observed spin-glass transitions. The nature of the chiral-glass ordered state as well as of the critical phenomena are different from those of the 3D Ising SG, with strong similarities to the system showing the one-step-like RSB, while its exact nature and physical origin have remained to be understood.

The numerical calculation was performed on the Fujitsu VPP500 at the supercomputer center, ISSP, University of Tokyo, on the HITACHI SR-2201 at the supercomputer center, University of Tokyo, and on the CP-PACS computer at the Center for Computational Physics, University of Tsukuba.

-
- [1] For reviews on spin glasses, see *e. g.*, (a) K. Binder and A. P. Young, *Rev. Mod. Phys.* **58** (1986) 801; (b) K. H. Fischer and J. A. Hertz, *Spin Glasses* Cambridge University Press (1991); (c) J. A. Mydosh, *Spin Glasses* Taylor & Francis (1993); (d) A. P. Young (*ed.*), *Spin glasses and random fields* World Scientific, Singapore (1997).
 - [2] J. A. Olive, A. P. Young and D. Sherrington, *Phys. Rev.* **B34**, 6341 (1986).
 - [3] H. Kawamura, *Phys. Rev. Lett.* **68** (1992) 3785.; *Int. Jour. Mod. Phys.* **7**, 345 (1996).
 - [4] H. Kawamura, *J. Phys. Soc. Jpn.* **64**, 26 (1995).
 - [5] H. Kawamura, *Phys. Rev. Lett.* **80**, 5421 (1998).
 - [6] F. Matsubara, T. Iyota, and S. Inawashiro, *Phys. Rev. Lett.* **67**, 1458 (1991).
 - [7] K. Hukushima and K. Nemoto, *J. Phys. Soc. Jpn.* **65**, 1604 (1996).
 - [8] H. Kawamura and M. Tanemura, *J. Phys. Soc. Jpn.* **60** (1991) 608.
 - [9] H. Kawamura, *Phys. Rev.* **B** 51 (1995)12398.
 - [10] J. Maucourt and D. R. Grempel, *Phys. Rev. Lett.* **80** (1998) 770.
 - [11] E. Marinari, C. Naitza, G. Parisi, M. Picco, F. Ritort and F. Zuliani, *Phys. Rev. Lett.* **81**, 1698 (1998).
 - [12] H. Bokil, A.J. Bray, B. Drossel and M.A. Moore, *cond-mat/9811080*.
 - [13] We have checked by numerical simulations that these features are indeed seen in the three-state mean-field Potts glass, a model exactly known to exhibit a one-step RSB; K. Hukushima and H. Kawamura, unpublished.